Article

The Local Structure of the BiS$_2$ Layer in RE(O,F)BiS$_2$ Determined by In-Plane Polarized X-ray Absorption Measurements

G. M. Pugliese [1], L. Tortora [1], E. Paris [1,2], T. Wakita [3], K. Terashima [3,4], A. Puri [5], M. Nagao [6], R. Higashinaka [7], T. D. Matsuda [7], Y. Aoki [7], T. Yokoya [3], T. Mizokawa [8] and N. L. Saini [1,*]

[1] Department of Physics, Sapienza University of Rome, P. le Aldo Moro 2, 00185 Roma, Italy; gianmarco.pugliese@uniroma1.it (G.M.P.); lorenzo.tortora@uniroma1.it (L.T.); eugenio.paris@psi.ch (E.P.);

[2] Photon Science Division, Swiss Light Source, Paul Scherrer Institut, 5232 Villigen, Switzerland

[3] Research Institute for Interdisciplinary Science (RIIS), Okayama University, Okayama 700-8530, Japan; wakita@cc.okayama-u.ac.jp (T.W.); TERASHIMA.Kensei@nims.go.jp (K.T.); yokoya@cc.okayama-u.ac.jp (T.Y.)

[4] National Institute for Materials Science, Sengen 1-2-1, Tsukuba 305-0047, Japan

[5] CNR-IOM-OGG c/o ESRF—The European Synchrotron, 71 Avenue des Martyrs, 38000 Grenoble, France; puri@esrf.fr

[6] Center for Crystal Science and Technology, University of Yamanashi, 7-32 Miyamae, Kofu 400-8511, Japan; mnagao@yamanashi.ac.jp

[7] Department of Physics, Tokyo Metropolitan University, 1-1, Minami-Osawa, Hachioji 192-0397, Japan; higashin@tmu.ac.jp (R.H.); tmatsuda@tmu.ac.jp (T.D.M.); aoki@tmu.ac.jp (Y.A.)

[8] Department of Applied Physics, Waseda University, Tokyo 169-8555, Japan; mizokawa@waseda.jp

* Correspondence: naurang.saini@roma1.infn.it

Abstract: We have investigated the local structure of BiS$_2$-based layered materials by Bi L$_3$-edge extended X-ray absorption fine structure (EXAFS) measurements performed on single crystal samples with polarization of the X-ray beam parallel to the BiS$_2$ plane. The results confirm highly instable nature of BiS$_2$ layer, characterized by ferroelectric like distortions. The distortion amplitude, determined by the separation between the two in-plane (Bi-S1) bonds, is found to be highest in LaO$_{0.77}$F$_{0.23}$BiS$_2$ with $\Delta R \sim 0.26$ Å and lowest in NdO$_{0.71}$F$_{0.29}$BiS$_2$ with $\Delta R \sim 0.13$ Å. Among the systems with intrinsic doping, CeOBiS$_2$ shows smaller distortion ($\Delta R \sim 0.15$ Å) than PrOBiS$_2$ ($\Delta R \sim 0.18$ Å) while the highest distortion appears for EuFBiS$_2$ revealing $\Delta R \sim 0.22$ Å. It appears that the distortion amplitude is controlled by the nature of the RE(O,F) spacer layer in the RE(O,F)BiS$_2$ structure. The X-ray absorption near edge structure (XANES) spectra, probing the local geometry, shows a spectral weight transfer that evolves systematically with the distortion amplitude in the BiS$_2$-layer. The results provide a quantitative measurements of the local distortions in the instable BiS$_2$-layer with direct implication on the physical properties of these materials.

Keywords: layered materials; local structure; X-ray absorption spectroscopy

1. Introduction

Layered materials have been a subject of intense research during these decades due to possibility of control and manipulation of their physical properties to obtain desired functions. The discovery of high T$_c$ superconductivity in layered copper oxides [1] had been one of the major breakthroughs and since then a large number of new layered materials have been found to show unconventional superconductivity. The research in the field was further fuelled by the discovery of superconductivity in the layered iron arsenides [2] resulting in several new layered systems. Among others, BiS$_2$-based systems [3,4] have received increasing attention during the last decade both for their superconducting and thermoelectric properties, leading to numerous theoretical and experimental studies to understand their functional properties [5–8]. The most studied BiS$_2$-based systems have been RE(O,F)BiS$_2$ (RE = rare earth element) in which twin BiS$_2$-layer is alternated by a RE(O,F) spacer layer in the crystallographic unit cell. The characteristic transport properties

of these materials are generally controlled by manipulating the electronic structure and crystal structure in different ways [5–7]. The parent REOBiS$_2$ is semiconducting and substitution of O^{2-} by F^{1-} in the REO layer introduces electrons in the BiS$_2$-layer that leads to superconductivity at low temperature with transition temperature depending on the nature of the spacer layer as well on the growth conditions [5–7]. The highest superconducting transition temperature T$_c$ ~10.5 K has been found in high pressure grown LaO$_{1-x}$F$_x$BiS$_2$ system.

Beyond electron doping by substitution in the REO spacer layer, the superconductivity in these materials has been manipulated by physical and chemical pressure. For example, isovalent substitutions in the REO-layer by RE^{3+} and in the BiS$_2$-layer by Se^{2-} (at of S^{2-}) have been exploited to optimise the transition temperature and the nature of the superconducting properties of these materials through the chemical pressure [9]. The isovalent substitution of S^{2-} by Se^{2-} in undoped LaOBiS$_2$ has also been used to manipulate the thermoelectric characteristics resulting a quality factor zT as high as ~0.36 at 650 K in LaOBiSSe [10,11]. Besides, it has been found that the mixed valent rare earth ion in the REO spacer layer can be a source of electron doping in the BiS$_2$ layer. This is known as self-doping, that is of particular interest since no external substitution is required and the self-doped system is free from any substitutional disorder. Indeed, self-doped superconductivity in EuFBiS$_2$ is known to occur due to mixed valence of Eu (Eu^{2+}/Eu^{3+}) [12]. Similarly, CeOBiS$_2$ has been found to show superconductivity due to self-doping introduced by the Ce^{3+}/Ce^{4+} mixed valence [13]. The examples also include other BiS$_2$-based superconductors in which RE mixed valence provides the self-doping [14–18] including in PrOBiS$_2$ [19].

One of the peculiar properties of the BiS$_2$-based superconductors is their structural instability. Indeed, BiS$_2$-layer in these materials has been found to be intrinsically instable [20–22] in the structure driven by the local Bi^{3+} defect chemistry and hence their physical properties can be easily manipulated by chemical and/or physical pressures. Experimental techniques sensitive to the local structure have revealed ferroelectric like distortions of BiS$_2$-layer to be prevalent that varies from system to system [23–26]. Furthermore, the local structure studies have also revealed the axial sulfur position with respect to Bi to play an important role in the physical properties [26,27]. Incidentally, all these local structural studies have been performed on polycrystalline samples and considering the highly susceptible nature of the BiS$_2$-layer under physical and/or chemical pressures a quantitative estimation of the local distortions can be challenging as it may depend on the sample morphology and growth conditions.

Here, we have measured the local structure of a series of RE(O,F)BiS$_2$ (RE = La, Eu, Pr, Ce, Nd) using single crystal samples to quantify the local distortions in the instable BiS$_2$-layer. For the purpose, we have studied two samples (LaO$_{0.77}$F$_{0.23}$BiS$_2$ and NdO$_{0.71}$F$_{0.29}$BiS$_2$) in which the doping is introduced by substitution while three samples are self-doped (EuFBiS$_2$, CeOBiS$_2$ and PrOBiS$_2$). The samples were chosen on the basis of their superconducting transition temperature at optimum doping and their crystal quality. The optimum doping in the LaO$_{1-x}$F$_x$BiS$_2$ and NdO$_{1-x}$F$_x$BiS$_2$ corresponds to x~0.25. The crystal quality was the factor for slightly different doping contents in the two systems but such a small difference hardly affects the transition temperature and the local structure. We have exploited Bi L$_3$-edge extended X-ray absorption fine structure measurement (EXAFS) with polarization of the X-ray beam parallel to the BiS$_2$-layer. The study has been carried out at low temperature (~20 K) on five different systems confirming that the BiS$_2$-layer of these materials is characterized by ferroelectric or quasi-ferroelectric like distortions of which magnitude depends on the nature of the RE(O,F) spacer layer. The single crystal of LaO$_{0.77}$F$_{0.23}$BiS$_2$ reveals largest distortion with ΔR~0.26 Å, while NdO$_{0.71}$F$_{0.29}$BiS$_2$ is characterized by the smallest distortion (ΔR~0.13 Å). Among self-doped systems, EuFBiS$_2$ with EuF-spacer layer reveals distortion amplitude ΔR~0.22 Å, substantially larger than the one in CeOBiS$_2$ (ΔR~0.15 Å) and PrOBiS$_2$ (ΔR~0.18 Å) with REO-spacer layer. The X-ray absorption near edge structure (XANES) spectra reveal a differing spectral weight that de-

pends on the distortion amplitude. We find that the local distortions amplitude measured on single crystal samples is systematically lower than the one reported on polycrystalline samples. The results provide a quantitative measurements of the local distortions in the instable BiS_2-layer of these materials.

2. Materials and Methods

Single crystals samples of $LaO_{0.77}F_{0.23}BiS_2$, $NdO_{0.71}F_{0.29}BiS_2$ and self-doped $EuFBiS_2$, $CeOBiS_2$ and $PrOBiS_2$ were grown by CsCl-based flux method [28–30]. A single-crystal X-ray analysis was performed revealing the average crystal structure to have the tetragonal space group P4/nmm with lattice parameters shown in Table 1. The samples were well characterized for their physical properties prior to the X-ray absorption measurements at the European Synchrotron Radiation Facility (ESRF) in Grenoble, France. The samples studied were all superconducting (except $EuFBiS_2$) showing zero resitivity below the transition temperature T_c shown in Table 1. Details on sample synthesis, growth and characterization are reported elsewhere [28–30]. Bi L_3-edge (13418 eV) X-ray absorption experiments were carried out in the normal incidence geometry in which the X-ray polarization is parallel to the ab-plane of the flat single crystal samples. Four samples ($LaO_{0.77}F_{0.23}BiS_2$, $NdO_{0.71}F_{0.29}BiS_2$, $EuFBiS_2$ and $CeOBiS_2$) were measured at the beamline BM23 while $PrOBiS_2$ was measured at BM08 using similar experimental set-up obtaining the X-ray absorption spectra in the fluorescence mode. In-plane polarized X-ray beam was monochromatized by a double crystal Si(111) monochromator and a 13-element Ge detector system was used for the fluorescence detection. A continuous flow He cryostat was used for the sample cooling and the measurements were carried out at 20 K with the sample temperature control within ± 1 K during the measurements. Four to five absorption scans were obtained on each sample for the spectral reproducibility. Standard procedure based on the spline fits [31,32] was used to extract EXAFS oscillations from the measured X-ray absorption spectra exploiting ATHENA software [33].

Table 1. Lattice parameters of the tetragonal unit cell (Space group P4/nmm) of different compounds. The transition temperatures (T_c) and in-plane distortion amplitudes (ΔR) are also included. ΔR_{sc} represents the separation between the two peaks in the pair distribution function derived in the present work while ΔR_p corresponds to the distortion amplitudes reported on polycrystalline samples.

	T_c (K)	a (Å)	c (Å)	ΔR_{sc} (Å)	ΔR_p (Å)
$LaO_{0.77}F_{0.23}BiS_2$	2.5	4.057	13.547	0.26	0.40
$EuFBiS_2$	-	4.051	13.560	0.22	0.26
$NdO_{0.71}F_{0.29}BiS_2$	5.1	3.996	13.464	0.13	0.18
$CeOBiS_2$	1.3	3.984	13.490	0.15	0.19
$PrOBiS_2$	3.5	4.010	13.824	0.18	0.21

3. Results and Discussion

Figure 1 shows the Bi L_3-edge EXAFS oscillations extracted from the in-plane polarized X-ray absorption spectra measured at 20 K on the single crystal samples of $LaO_{0.77}F_{0.23}BiS_2$, $EuFBiS_2$, $PrOBiS_2$, $CeOBiS_2$ and $NdO_{0.71}F_{0.29}BiS_2$. The EXAFS oscillations are multiplied by k^2 to enhance the spectral amplitude at higher k. The differing EXAFS oscillations indicate that the local structure has strong rare-earth dependence in $RE(O/F)BiS_2$. The crystal unit cell of $RE(O/F)BiS_2$ is also included for a ready reference. Large differences in the EXAFS oscillations indicate that the local structure evolves significantly with the RE(O/F)-layer. The oscillations for $k \leq 8$ Å^{-1} are largely damped in $LaO_{0.77}F_{0.23}BiS_2$ and $EuFBiS_2$ due to larger distortions involving nearest neighbors sulfur atoms around the photoabsorbing Bi (i.e., Bi-S1 bonds). Incidentally, self-doped systems ($EuFBiS_2$, $PrOBiS_2$, $CeOBiS_2$) show relatively damped oscillations for $k \geq 10$ Å^{-1}, likely to be related with mixed valence of the RE atoms since the higher k-oscillations are sensitive to the heavier atoms.
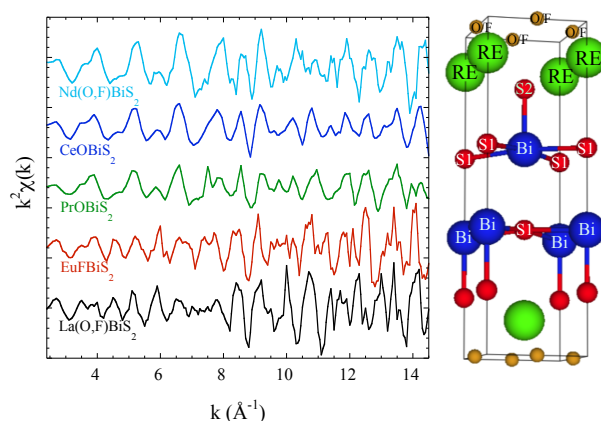
Figure 1. EXAFS oscillations of RE(O/F)BiS$_2$ single crystals samples (RE = La, Eu, Pr, Ce, Nd) measured at Bi L$_3$-edge with X-ray polarization parallel to the crystallographic ab-plane. The oscillations are weighed by k^2 to amplify the signal at higher k-values and vertically shifted for a better visualization. The crystal unit cell of RE(O/F)BiS$_2$ is also shown.

The Fourier Transform (FT) magnitude of the k^2-weighted EXAFS oscillations is shown in Figure 2, providing real-space information on the local atomic distribution around the photoabsorbing Bi. In the RE(O/F)BiS$_2$ structure, the Bi atom is coordinated with one axial sulfur atom (S2) and one sulfur of the twin BiS$_2$ layer, however, their contributions are minimum in the EXAFS measured with polarization parallel to the crystallographic ab-plane. Therefore, the nearest neighbor contribution, at 2–3 Å, is mainly coming from the four in-plane sulfur atoms (S1) since the polarization vector of the X-ray beam **ê** ∥ *ab* plane [32,34]. The contribution appears as peak structures in the FT magnitude at ∼2.5 Å. The peak structure ∼4 Å is mainly due to the Bi-Bi bonds within the plane, representing the in-plane lattice parameter in RE(O/F)BiS$_2$ structure. Apparently the Bi-Bi peak shifts and follows the in-plane lattice behavior in the tetragonal RE(O/F)BiS$_2$ structure. The lattice parameters of the studied crystals are summarized in Table 1 [28–30,35]. The distant peaks beyond ∼4 Å include contribution of Bi-RE and diagonal Bi-Bi distances including also multiple scattering contributions.

Here the aim is to quantify the distortions in the BiS$_2$-layer and for the purpose the contribution of Bi-S1 was Fourier filtered in the R-window (1.5–3.5 Å) shown as shadowed region in Figure 2. The shapes of filtered EXAFS oscillations, shown in Figure 3 (inset), are significantly different between them indicating that the local Bi-S1 distribution in RE(O/F)BiS$_2$ evolves largely with RE(O/F)-spacer layer. We have evaluated the pair distribution function (PDF) of the Bi-S1 bonds from the analysis of the filtered EXAFS. The EXCURVE 9.275 code (with calculated phase shift functions and backscattering amplitudes) was used for extracting the PDF [36] starting from a model containing a distribution of harmonic oscillators describing the Bi-S pairs. The final Bi-S1 distribution was merged in a two peak function for all the samples (Figure 3) confirming that BiS$_2$-layer in these materials is characterized by a ferroelectric or quasi ferroelectric-like distortion [20–22]. Similar Bi-S1 distribution was obtained by constrained EXAFS model fits in which residual contribution of axial Bi-S2 bonds was included together with the in-plane Bi-S1 bonds respecting the effective number of near neighbors expected from the polarization dependence of L$_3$-edge EXAFS [32,34]. The corresponding theoretical signals are included as solid lines with the filtered EXAFS as insets. It is worth mentioning that such a distortion corresponds to atomic displacement within the BiS$_2$-layer. On the basis of first principles calculations a spontaneous in-plane ferroelectric polarization has been suggested [37].
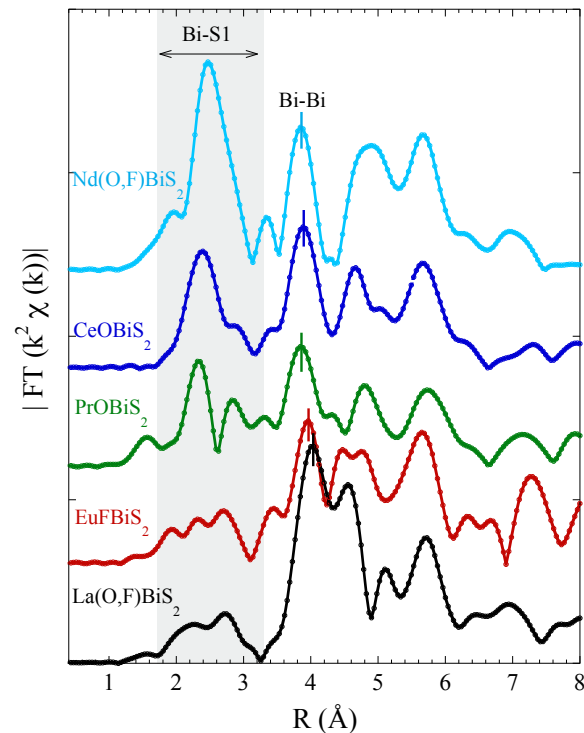
Figure 2. Fourier transforms (FT) magnitudes of Bi L_3-edge k^2-weighted EXAFS oscillations for RE(O/F)BiS$_2$ at 20 K. The FTs are performed using a Gaussian window in the k-range of 3–14.5 Å^{-1}.

One can make several observations from the PDF shown in Figure 3. The largest distortion amplitude, defined by the separation between the two peaks (ΔR) of the distribution, is found to be for La(O/F)BiS$_2$ (see, e.g., the vertical dotted lines in Figure 3). The distribution is quasi ferroelectric-like with differing weight of the two Bi-S1 bonds. Incidentally, the distortion amplitude of ΔR∼0.26 Å is smaller than the one found in polycrystalline samples reporting ΔR∼0.4 Å by neutron pair distribution function (PDF) analysis [23] and by EXAFS analysis [24]. On the other hand Nd(O/F)BiS$_2$ reveals smallest distortion amplitude (ΔR∼0.13 Å) with the distortion being quasi ferroelectric-like. Again, the distortion amplitude is significantly lower than the one reported by neutron PDF on polycrystalline sample showing ΔR to be ∼0.18 Å [25]. Among the self-doped BiS$_2$ systems, EuFBiS$_2$ shows almost equal probability of the two bonds indicating ferroelectric-like distortion. The distortion amplitude for EuFBiS$_2$ (ΔR∼0.22 Å) is lower than what has been reported in polycrystalline sample of the same system (ΔR∼0.26 Å) measured by EXAFS [26]. The self-doped system PrOBiS$_2$ also appears with ferroelectric-like distortion although the amplitude (ΔR∼0.18 Å) is lower than the one in EuFBiS$_2$. Similarly, the distribution in CeOBiS$_2$ is quasi ferroelectric-like, that is smallest among the self-doped systems (ΔR∼0.15 Å). Again, the distortion amplitude is lower than the one found in polycrystalline samples CeOBiS$_2$ (ΔR∼0.19 Å). This seems plausible due to the fact that the ground state of these materials is highly susceptible to the external conditions and one can expect the morphology of the system to have substantial effect on the distortion amplitude as well. It should be mentioned that the mean Bi-S1 distance, estimated by the weighted average of the PDF, is consistent with the one measured by diffraction experiments [28–30,35]. It is also worth noting that the distortion evolves with c-axis of the system and hence the axial coupling may have some important role in these materials.

Apparently, there is no direct correlation between the superconducting transition temperature and the Bi-S1 distortion amplitude in the studied samples. However, if we compare La(O/F)BiS$_2$ and Nd(O/F)BiS$_2$, the less distorted system tends to have higher T_c. Indeed, La(O/F)BiS$_2$, showing highest distortion amplitude, is superconducting with T_c∼2.5 K while Nd(O/F)BiS$_2$ with lowest distortion amplitude shows T_c∼5.1 K. However,

among the self-doped systems, PrOBiS$_2$ is superconducting at T$_c$~3.5 K with distortion amplitude larger than that in CeOBiS$_2$ showing superconductivity at lower temperature (T$_c$~1.3 K). Unlike the above, the self-doped EuFBiS$_2$ with EuF spacer layer is non-superconducting down to 0.15 K and reveals substantial distortion in compare to other self-doped systems with REO spacer layer (PrOBiS$_2$ and CeOBiS$_2$). Therefore, although the T$_c$ is affected by in-plane distortions, a direct relationship can not be argued. Here, it is worth mentioning that in the self-doped systems, if the carriers provided by the mixed valence of the rare-earth ions are trapped by the out-of-plane Bi 6p$_z$ orbitals, the in-plane Bi 6p$_{x,y}$ orbitals are less populated and the strong in-plane distortion can still survive with superconductivity.
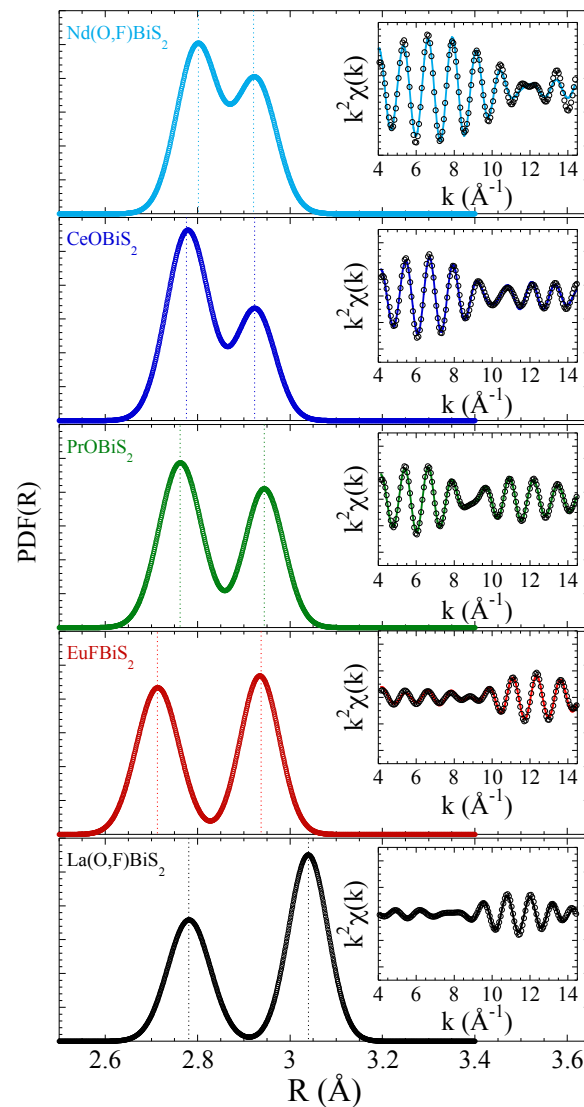
Figure 3. Bi-S1 bonds distribution functions obtained by in-plane polarized EXAFS measured on single crystal samples of RE(O/F)BiS$_2$. The insets show the Fourier filtered EXAFS oscillations (symbols) compared with the theoretical EXAFS (solid line) corresponding to the plotted distributions.

X-ray absorption near edge structure (XANES) probes higher order atomic correlation function, thus highly sensitive and useful probe of the local geometry and the valence electronic states [31,32]. The Bi L$_3$-edge XANES spectra measured at 20 K on single crystal samples of RE(O/F)BiS$_2$ are shown in Figure 4. The spectra are normalized with respect to the atomic absorption estimated by standard procedure based on a linear fit to the EXAFS region. Here, the spectrum of PrOBiS$_2$ is not included for the comparison considering

different experimental set-up and spectral resolution. The spectra show different spectral features and the nearest edge peak features are denoted by A and B. These features are related to the dipole allowed transition from Bi 2*p* to the unoccupied Bi 6*d* states in the continuum, admixed with the unoccupied Bi 6*p* states [31,32]. The latter are also hybridized with Bi 6*s* and S 3*p* states due to Bi^{3+} defect chemistry [38,39]. Therefore these peaks are sensitive probe of the local geometry around the photoabsorbing Bi.
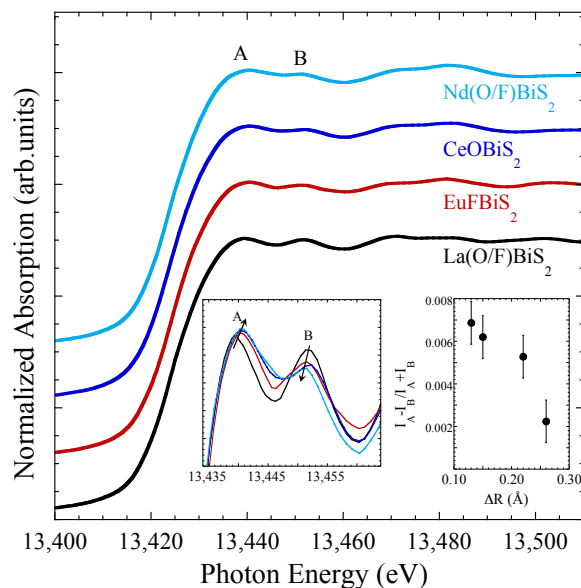
Figure 4. X-ray absorption near edge structure (XANES) spectra of RE(O/F)BiS$_2$ single crystals measured at the Bi L$_3$-edge. The nearest edge features are denoted by A and B. The left inset shows a zoom-over the features A and B. The right inset shows normalized intensity difference plotted as a function of the distortion amplitude in the BiS$_2$-layer. The error bars represent maximum uncertainty estimated by analyzing different scans for each sample.

The differences in the XANES features can be seen in the inset displaying a zoom-over the peaks A and B. Apparently, the peak A moves towards higher energy from La(O/F)BiS$_2$ to Nd(O/F)BiS$_2$ while the peak B tending to shift towards lower energy with an exchange of the spectral weight. Here, the spectral weight transfer is estimated by normalized intensity difference between the two peak features ($I_A - I_B/I_A + I_B$) and plotted as a function of the distortion amplitude determined by EXAFS (Figure 3) and shown in the inset (right) of Figure 4. The intensity difference shows a gradual decrease as a function of the distortion in the BiS$_2$-layer. Although, due to complexity of the distortions in these materials, it is difficult to establish a quantitative correlation between the distortions and the spectral weight transfer in the XANES spectra, the observed change in the local geometry can be taken as a marker for the local distortions.

4. Conclusions

In summary, the local distortions in RE(O/F)BiS$_2$ have been determined by Bi L$_3$-edge EXAFS measured on single crystal samples with polarization of the X-ray to be parallel to the BiS$_2$ layer. The BiS$_2$ layer is characterized by a two peak distribution function confirming ferroelectric-like nature of the local distortions in these materials. The distortion is largest for La(O/F)BiS$_2$ and shows a substantial change with the RE(O/F)-spacer layer appearing smallest in the case of Nd(O/F)BiS$_2$. The self-doped EuFBiS$_2$ shows a significantly larger distortion than other self-doped systems, namely PrOBiS$_2$ and CeOBiS$_2$. The distortion amplitude, measured on single crystal samples using polarized EXAFS, is systematically lower than the one found in polycrystalline samples. This is likely to be due to highly susceptible nature of BiS$_2$-based materials. Apparently, we do not

observe any quantitative correlation between the local distortions in the instable BiS$_2$-layer and the superconductivity. It is likely that in-plane distortions are responsible for the charge fluctuations in the BiS$_2$-layer with axial displacements having a crucial role in controlling the electronic transport properties of these materials.

Author Contributions: Conceptualization, N.L.S., T.M., T.Y. and Y.A.; methodology, E.P., T.W., A.P., K.T., R.H., T.D.M., M.N.; formal analysis, G.M.P. and L.T.; writing—original draft preparation, G.M.P. and N.L.S. All authors have read and agreed to the published version of the manuscript.

Institutional Review Board Statement: Not applicable.

Informed Consent Statement: Not applicable.

Data Availability Statement: The data presented in this study are available on reasonable request from the corresponding author.

Conflicts of Interest: The authors declare no conflict of interest.

References

1. Bednorz, J.G.; M*ü*ller, K.A. Possible high T$_c$ superconductivity in the Ba-La-Cu-O system. *Z. Phys. B* **1986**, *64*, 189. [CrossRef]
2. Kamihara, Y.; Watanabe, T.; Hirano, M.; Hosono, H. Iron-Based Layered Superconductor La[O$_{1-x}$F$_x$]FeAs (x= 0.05-0.12) with T$_c$ 26 K. *J. Am. Chem. Soc.* **2008**, *130*, 3296. [CrossRef] [PubMed]
3. Mizuguchi, Y.; Fujihisa, H.; Gotoh, Y.; Suzuki, K.; Usui, H.; Kuroki, K.; Demura, S.; Takano, Y.; Izawa, H.; Miura, O. BiS$_2$-based layered superconductor Bi$_4$O$_4$S$_3$. *Phys. Rev. B* **2012**, *86*, 220510(R). [CrossRef]
4. Mizuguchi, Y.; Demura, S.; Deguchi, K.; Takano, Y.; Fujihisa, H.; Gotoh, Y.; Izawa, H.; Miura, O. Superconductivity in Novel BiS$_2$-based Layered Superconductors LaO$_{1-x}$F$_x$BiS$_2$. *J. Phys. Soc. Jpn.* **2012**, *81*, 114725. [CrossRef]
5. Mizuguchi, Y. Review of superconductivity in BiS$_2$-based layered materials. *J. Phys. Chem. Sol.* **2015**, *84*, 34. [CrossRef]
6. Yazici, D.; Jeon, I.; White, B.D.; Maple, M.B. Superconductivity in layered BiS$_2$-based compounds. *Phys. Supercond. Its Appl.* **2015**, *514*, 218. [CrossRef]
7. Mizuguchi, Y. Material Development and Physical Properties of BiS$_2$-Based Layered Compounds. *J. Phys. Soc. Jpn.* **2019**, *88*, 041001. [CrossRef]
8. Suzuki, K.; Usui, H.; Kuroki, K.; Nomoto, T.; Hattori, K.; Ikeda, H. Electronic Structure and Superconducting Gap Structure in BiS$_2$-based Layered Superconductors. *J. Phys. Soc. Jpn.* **2019**, *88*, 041008. [CrossRef]
9. Mizuguchi, Y.; Miura, A.; Kajitani, J.; Hiroi, T.; Miura, O.; Tadanaga, K.; Kumada, N.; Magome, E.; Moriyoshi, C.; Kuroiwa, Y. In-plane chemical pressure essential for superconductivity in BiCh$_2$-based (Ch: S, Se) layered structure. *Sci. Rep.* **2015**, *5*, 14968. [CrossRef]
10. Nishida, A.; Miura, O.; Lee, C.H.; Mizuguchi, Y. High thermoelectric performance and low thermal conductivity of densified LaOBiSSe. *Appl. Phys. Express* **2015**, *8*, 111801. [CrossRef]
11. Nishida, A.; Nishiate, H.; Lee, C.H.; Miura, O.; Mizuguchi, Y. Electronic Origins of Large Thermoelectric Power Factor of LaOBiS$_{2-x}$Se$_x$. *J. Phys. Soc. Jpn.* **2016**, *85*, 074702. [CrossRef]
12. Guo, C.Y.; Chen, Y.; Smidman, M.; Chen, S.A.; Jiang, W.B.; Zhai, H.F.; Wang, Y.F.; Cao, G.H.; Chen, J.M.; Lu, X.; et al. Evidence for two distinct superconducting phases in EuFBiS$_2$ under pressure. *Phys. Rev. B* **2015**, *91*, 214512. [CrossRef]
13. Nagao, M.; Miura, A.; Ueta, I.; Watauchi, S.; Tanaka, I. Superconductivity in CeOBiS$_2$ with cerium valence fluctuation. *Solid State Comm.* **2016**, *245*, 11. [CrossRef]
14. Zhai, H.F.; Zhang, P.; Wu, S.Q.; He, C.Y.; Tang, Z.T.; Jiang, H.; Sun, Y.L.; Bao, J.K.; Nowik, I.; Felner, I.; et al. Anomalous Eu Valence State and Superconductivity in Undoped Eu$_3$Bi$_2$S$_4$F$_4$. *J. Am. Chem. Soc.* **2014**, *136*, 15386. [CrossRef]
15. Luo, Y.; Zhai, H.F.; Zhang, P.; Xu, Z.A.; Cao, G.H.; Thompson, J.D. Pressure-enhanced superconductivity in Eu$_3$Bi$_2$S$_4$F$_4$. *Phys. Rev. B* **2014**, *90*, 220510(R). [CrossRef]
16. Haque, Z.; Thakur, G.S.; Selvan, G.K.; Block, T.; Janka, O.; Pottgen, R.; Joshi, A.G.; Parthasarathy, R.; Mugam, S.A.; Gupta, L.C.; et al. Valence State of Eu and Superconductivity in Se-Substituted EuSr$_2$Bi$_2$S$_4$F$_4$ and Eu$_2$SrBi$_2$S$_4$F$_4$. *Inorg. Chem.* **2018**, *57*, 37. [CrossRef] [PubMed]
17. Haque, Z.; Thakur, G.S.; Parthasarathy, R.; Gerke, B.; Block, T.; Heletta, L.; Pottgen, R.; Joshi, A.G.; Selvan, G.K.; Arumugam, S.; et al. Unusual Mixed Valence of Eu in Two Materials: EuSr$_2$Bi$_2$S$_4$F$_4$ and Eu$_2$SrBi$_2$S$_4$F$_4$: Mössbauer and X-ray Photoemission Spectroscopy Investigations. *Inorg. Chem.* **2017**, *56*, 3182. [CrossRef]

18. Zhai, H.F.; Tang, Z.T.; Jiang, H.; Xu, K.; Zhang, K.; Zhang, P.; Bao, J.K.; Sun, Y.L.; Jiao, W.H.; Nowik, I.; et al. Possible charge-density wave, superconductivity, and f-electron valence instability in EuBiS$_2$F. *Phys. Rev. B* **2014**, *90*, 064518. [CrossRef]

19. Morita, T.; Matsuzawa, Y.; Kumar, S.; Schwier, E.F.; Shimada, K.; Higashinaka, R.; Matsuda, T.D.; Aoki, Y.; Saini, N.L.; Mizokawa, T. Evolution of the Fermi surface in superconductor PrO$_{1-x}$F$_x$BiS$_2$ (x= 0.0, 0.3,and 0.5) revealed by angle-resolved photoemission spectroscopy. *Phys. Rev. B* **2021**, *103*, 094510. [CrossRef]

20. Yildirim, T. Ferroelectric soft phonons, charge density wave instability, and strong electron-phonon coupling in BiS$_2$ layered superconductors: A first-principles study. *Phys. Rev. B.* **2013**, *87*, 020506(R). [CrossRef]

21. Liu, Q.; Zhang, X.; Zunger, A. Polytypism in LaOBiS2-type compounds based on different three-dimensional stacking sequences of two-dimensional *BiS$_2$* layers. *Phys. Rev. B* **2016**, *93*, 174119. [CrossRef]

22. Zhou, X.; Liu, Q.; Waugh, J.A.; Li, H.; Nummy, T.; Zhang, X.; Zhu, X.; Cao, G.; Zunger, A.; Dessau, D.S. Predicted electronic markers for polytypes of *LaOBiS$_2$* examined via angle-resolved photoemission spectroscopy. *Phys. Rev. B* **2017**, *95*, 075118. [CrossRef]

23. Athauda, A.; Yang, J.; Lee, S.; Mizuguchi, Y.; Deguchi, K.; Takano, Y.; Miura, O.; Louca, D. Charge Fluctuations in the NdO$_{1-x}$F$_x$BiS$_2$ Superconductors. *Phys. Rev. B* **2015**, *91*, 144112. [CrossRef]

24. Paris, E.; Mizuguchi, Y.; Wakita, T.; Terashima, K.; Yokoya, T.; Mizokawa, T.; Saini, N.L. Suppression of structural instability in *LaOBiS$_{2-x}$Se$_x$* by Se substitution. *J. Phys. Cond. Matt.* **2018**, *30*, 455703. [CrossRef] [PubMed]

25. Athauda, A.; Louca, D. Nanoscale Atomic Distortions in the *BiS$_2$* Superconductors: Ferrodistortive Sulfur Modes. *J. Phys. Soc. Jpn.* **2019**, *88*, 041004. [CrossRef]

26. Pugliese, G.M.; Paris, E.; Capone, F.G.; Stramaglia, F.; Wakita, T.; Terashima, K.; Yokoya, T.; Mizokawa, T.; Mizuguchi, Y.; Saini, N.L. The local structure of self-doped *BiS$_2$*-based layered systems as a function of temperature. *Phys. Chem. Chem. Phys.* **2020**, *22*, 22217. [CrossRef] [PubMed]

27. Pugliese, G.M.; Stramaglia, F.; Capone, F.G.; Hacisalihoglu, M.Y.; Kiyama, R.; Sogabe, R.; Goto, Y.; Pollastri, S.; Souza, D.O.D.; Olivi, L.; et al. Local structure displacements in La$_{1-x}$Ce$_x$OBiSSe as a function of Ce concentration. *J. Phys. Chem. Solids* **2020**, *147*, 109648. [CrossRef]

28. Nagao, M. Growth and characterization of *R(O, F)BiS$_2$* (R = La, Ce, Pr, Nd) superconducting single crystals. *Nov. Supercond. Mater.* **2019**, *1*, 64. [CrossRef]

29. Higashinaka, R.; Asano, T.; Nakashima, T.; Fushiya, K.; Mizuguchi, Y.; Miura, O.; Matsuda, T.D.; Aoki, Y. J. Symmetry Lowering in *LaOBiS$_2$*: A Mother Material for *BiS$_2$*-Based Layered Superconductors. *Phys. Soc. Jpn.* **2015**, *84*, 023702. [CrossRef]

30. Sugimoto, T.; Paris, E.; Terashima, K.; Barinov, A.; Giampietri, A.; Wakita, T.; Yokoya, T.; Kajitani, J.; Higashinaka, R.; Matsuda, T.D.; et al. Inhomogeneous charge distribution in a self-doped *EuFBiS$_2$* superconductor. *Phys. Rev. B* **2019**, *100*, 064520. [CrossRef]

31. Koningsberger, D.C.; Prins, R. X-ray Absorption: Principles, Applications, Techniques of EXAFS, SEXAFS and XANES. In *Chemical Analysis: A Series of Monographs on Analytical Chemistry and Its Applications*; Wiley: Hoboken, NJ, USA, 1988.

32. Bunker, G. *Introduction to XAFS*; Cambridge University Press: Cambridge, UK, 2010.

33. Ravel, B.; Newville, M. ATHENA, ARTEMIS, HEPHAESTUS: Data analysis for X-ray absorption spectroscopy using IFEFFIT. *J. Synch. Rad.* **2005**, *12*, 537. [CrossRef] [PubMed]

34. Brouder, C. Angular dependence of X-ray absorption spectra. *J. Phys. Condens. Matter* **1990**, *2*, 701. [CrossRef]

35. Miura, A.; Nagao, M.; Takei, T.; Watauchi, S.; Tanaka, I.; Kumada, N. Crystal structure of LaO$_{1-x}$F$_x$BiS$_2$ (x∼0.23, 0.46): Effect of F doping on distortion of Bi-S plane. *J. Solid State Chem.* **2014**, *212*, 213. [CrossRef]

36. Gurman, S.J. Interpretation of EXAFS Data. *J. Synchrotron Radiat.* **1995**, *2*, 56. [CrossRef] [PubMed]

37. He, C.; Zhu, J.; Zhao, Y.-H.; Liu, C.; Fu, B. Unconventional inner-TL electric polarization in TL-*LaOBiS$_2$* with ultrahigh carrier mobility. *Nanoscale* **2019**, *11*, 18436. [CrossRef] [PubMed]

38. Du, Y.; Ding, H.C.; Sheng, L.; Savrasov, S.Y.-; Wan, X.; Duan, C.G. Microscopic origin of stereochemically active lone pair formation from orbital selective external potential calculations. *J. Phys. Condens. Matter* **2014**, *26*, 025503. [CrossRef] [PubMed]

39. Rathore, E.; Juneja, R.; Culver, S.P.; Minafra, N.; Singh, A.K.; Zeier, W.G.; Biswas, K. Origin of Ultralow Thermal Conductivity in n-Type Cubic Bulk *AgBiS$_2$*: Soft Ag Vibrations and Local Structural Distortion Induced by the *Bi6s^2* Lone Pair. *Chem. Mater.* **2019**, *31*, 2106. [CrossRef]